Boundary-Layer Meteorology (2006) 119: 473–500
DOI 10.1007/s10546-005-9036-2

REVISITING THE LOCAL SCALING HYPOTHESIS IN STABLY STRATIFIED ATMOSPHERIC BOUNDARY-LAYER TURBULENCE: AN INTEGRATION OF FIELD AND LABORATORY MEASUREMENTS WITH LARGE-EDDY SIMULATIONS

SUKANTA BASU[1,*], FERNANDO PORTÉ-AGEL[1], EFI FOUFOULA-GEORGIOU[1], JEAN-FRANÇOIS VINUESA[1] and MARKUS PAHLOW[2]

[1]*St. Anthony Falls Laboratory, University of Minnesota, Minneapolis, MN 55414, U.S.A;* [2]*Institute of Hydrology, Water Resources Management and Environmental Engineering, Ruhr-University Bochum, 44780 Bochum, Germany*

(Received in final form 26 September 2005 / Published online: 20 December 2005)

Abstract. The 'local scaling' hypothesis, first introduced by Nieuwstadt two decades ago, describes the turbulence structure of the stable boundary layer in a very succinct way and is an integral part of numerous local closure-based numerical weather prediction models. However, the validity of this hypothesis under very stable conditions is a subject of ongoing debate. Here, we attempt to address this controversial issue by performing extensive analyses of turbulence data from several field campaigns, wind-tunnel experiments and large-eddy simulations. A wide range of stabilities, diverse field conditions and a comprehensive set of turbulence statistics make this study distinct.

Keywords: Intermittency, Large-eddy simulation, Local scaling, Monin–Obukhov similarity theory, Stable boundary layer, Turbulence.

Glossary of Symbols

f_c	Coriolis parameter
g	gravitational acceleration
G	geostrophic wind speed
H	boundary-layer height
L	Obukhov length $(=-\Theta u_*^3/\kappa g(\overline{w\theta}))$
r_{mn}	correlation coefficient between m and n
u, v, w	velocity fluctuations (around the average) in x, y and z directions
U, V	mean velocity components in x and y directions
u_*	friction velocity $\left(=\sqrt[4]{\overline{uw}^2+\overline{vw}^2}\right)$
$\overline{uw}, \overline{vw}$	vertical turbulent momentum fluxes
$\overline{u\theta}, \overline{w\theta}$	longitudinal and vertical heat fluxes

* E-mail: sukanta.basu@ttu.edu

z height above the surface
κ von Karman constant ($=0.40$)
Λ local Obukhov length
σ_m standard deviation of m
θ temperature fluctuations (around the average)
Θ mean temperature
θ_* temperature scale ($=-\overline{w\theta}/u_*$)
ζ stability parameter ($=z/\Lambda$)

A subscript '$_L$' on the turbulence quantities (e.g., u_{*L}) will be used to specify evaluation using local turbulence quantities – otherwise, surface values are implied.

1. Introduction

In comparison with convective and neutral atmospheric boundary-layer (ABL) turbulence, stable boundary layer (SBL) turbulence has not received much attention despite its scientifically intriguing nature and practical significance (e.g., in numerical weather prediction – NWP, and pollutant transport). This might be attributed to the lack of adequate field or laboratory measurements, to the inevitable difficulties in numerical simulations (arising from small scales of motion due to stratification), and to the intrinsic complexities in its dynamics (e.g., occurrences of intermittency, Kelvin–Helmholtz instability, gravity waves, low-level jets, meandering motions, etc.) (Hunt et al., 1996; Mahrt, 1998a; Derbyshire, 1999).

Fortunately, the contemporary literature is witnessing a brisk surge in the reporting of SBL turbulence research. Field campaigns such as SABLES 98 (Stable Atmospheric Boundary-Layer Experiment in Spain, 1998) (Cuxart et al., 2000), CASES-99 (Cooperative Atmosphere-Surface Exchange Study, 1999) (Poulos et al., 2002) and high-quality wind-tunnel experiments (Ohya et al., 1997; Ohya, 2001) geared towards comprehensive investigation of the SBL are being carried out. In the case of numerical modelling, a handful of partially successful large-eddy simulations (LESs) were also attempted during the last decade (Mason and Derbyshire, 1990; Brown et al., 1994; Andrén, 1995; Galmarini et al., 1998; Kosović and Curry, 2000; Saiki et al., 2000; Ding et al., 2001; Beare and MacVean, 2004). Very recently, the first intercomparison of several LES models for the SBL has been conducted as a part of the GABLS (Global Energy and Water Cycle Experiment Atmospheric Boundary Layer Study) initiative (Holtslag, 2003; Beare et al., 2006). In the past, direct numerical simulations (DNS) of stable shear flows were also attempted (see Barnard (2000) and the references therein). However, very low Reynolds number ($Re \sim 10^3$) of these simulations make their applicability to ABL flows ($Re \sim 10^7$) questionable. In a parallel line of research, various tools borrowed from the dynamical systems theory have also been applied to SBL turbulence during

this period (Revelle, 1993; McNider et al., 1995; Basu et al., 2002; van de Wiel, 2002).

Despite all these synergistic efforts in understanding the SBL, several unresolved (seemingly controversial) issues still remain. It is the purpose of this paper to address one such unresolved issue: the validity of Nieuwstadt's 'local scaling' hypothesis (Nieuwstadt, 1984a,b, 1985; Derbyshire, 1990) in the very stable atmospheric boundary layer.

To achieve this goal, we performed extensive analyses of turbulence data from several field campaigns with diverse field conditions. Further support for our claims is provided by analyzing datasets from wind-tunnel experiments (Ohya, 2001) and also simulated by a new generation LES (Porté-Agel et al., 2000; Porté-Agel, 2004; Basu, 2004; Stoll and Porté-Agel, 2006). It is important to stress that a combination of statistical analyses of field measurements, laboratory data and numerical simulations was essential for this research. Used in a complementary fashion, they increased the reliability of our findings by reducing uncertainties inherent to all the techniques. For instance, in the stable atmospheric boundary layer, the presence of mesoscale variabilities of unknown origin is ubiquitous. Such mesoscale motions might complicate the comparisons between observational and theoretically anticipated statistics. On the other hand, information from controlled wind-tunnel experiments are 'pristine' in the sense that the measurements are neither subject to subgrid-scale (SGS) parameterization errors nor corrupted by mesoscale variabilities. However, a wind tunnel might never be able to simulate the complexities of the atmosphere including the very high Reynolds number of atmospheric flows. LES overcomes most of the aforementioned problems but is susceptible to the SGS parameterization issues.

2. Background

Over land, stable conditions are usually characteristic of the nocturnal boundary layer (NBL), but can also persist for several months in polar regions during winter (Kosović and Curry, 2000; Holtslag, 2003). During stable stratification, turbulence is generated by mechanical shear and destroyed by (negative) buoyancy force and viscous dissipation (Stull, 1988; Arya, 2001). This inhibition by the buoyancy force tends to limit the vertical extent of turbulent mixing, and implies that the boundary layer height (H) is not an appropriate length scale in the SBL. In his local scaling hypothesis, Nieuwstadt (1984a,b, 1985) conjectured that under stable stratification the local Obukhov length (Λ), based on local turbulent fluxes, should be considered as a more fundamental length scale. Then, according to this hypothesis, dimensionless combinations of turbulent variables (gradients, fluxes, (co-)variances, etc.) that are measured at the same height (z)

could be expressed as 'universal' functions of a single scaling parameter $\zeta(=z/\Lambda)$, known as the stability parameter. Exact forms of these functions could be predicted by dimensional analysis only in the asymptotic very stable case ($\zeta \to \infty$), as discussed below.

During clear nights with weak winds, the land surface cools due to strong longwave radiative cooling and the overlying boundary layer may become very stable. Typically, when a surface cools, the heat diffusion increases and compensates for the cooling. But, under very stable conditions, due to less efficient vertical mixing associated with strong stratification, the downward turbulent heat flux is very small – resulting in an even colder surface and the boundary layer becomes increasingly more stable (a positive feedback effect). At some point, turbulent exchange between the surface and the atmosphere ceases and the boundary layer becomes decoupled from the surface (Beljaars and Viterbo, 1998; Viterbo et al., 1999; Mahrt and Vickers, 2002). Wyngaard (1973) coined the term 'z-less stratification' for this unique decoupling phenomenon. In this very stable regime, any explicit dependence on z disappears and as a consequence local scaling predicts that dimensionless turbulent quantities asymptotically approach constant values (Nieuwstadt, 1984a,b, 1985).

Local scaling could be viewed as a generalization of the well-established Monin–Obukhov (M–O) similarity theory (Monin and Yaglom, 1971; Sorbjan, 1989). M–O similarity theory is strictly valid in the surface layer (lowest 10% of the ABL), whereas local scaling describes the turbulent structure of the entire SBL (Nieuwstadt, 1984a,b, 1985). This means that by virtue of local scaling, field observations from the surface layer and the outer layer could be combined for statistical analysis. For large-scale NWP models with local closure this would also mean that the closure scheme for the surface layer and the outer layer could be the same (Beljaars, 1992).

Recently, Pahlow et al. (2001) questioned the validity of the concept of M–O similarity theory (and thus the local scaling hypothesis) under very stable stratification. Local scaling is a powerful reductionist approach to the SBL (Brown et al., 1994) and is an integral part of numerous local-closure based present-day NWP models. Thus, in our opinion, it is worth revisiting and attempting to reconcile any controversy regarding its validity.

3. Description of Data

We primarily made use of an extensive atmospheric boundary-layer turbulence dataset (comprising of fast-response sonic anemometer data) collected by various researchers from the Johns Hopkins University, the University of California-Davis and the University of Iowa during Davis 1994, 1995, 1996, 1999 and Iowa 1998 field studies. Comprehensive descriptions of

these field experiments (e.g., surface cover, fetch, instrumentation, sampling frequency) can be found in Pahlow et al. (2001). We further augmented this dataset with NBL turbulence data from CASES-99, a cooperative field campaign conducted near Leon, Kansas during October 1999 (Poulos et al., 2002). For our analyses, data from sonic anemometers located at four levels (1.5, 5, 10 and 20 m) on the 60-m tower and the adjacent mini-tower collected during two intensive observational periods (nights of October 17 and 19) were considered (the sonic anemometer at 1.5 m was moved to 0.5 m level on October 19). Briefly, the collective attributes of the field dataset explored in this study are as follows: (i) surface cover: bare soil, grass and beans; (ii) sampling frequency: 18–60 Hz; (iii) sampling period: 20–30 min; (iv) sensor height (z): 0.5–20 m; and (v) atmospheric stability (ζ) :≈ 0 (neutral) to ≈ 10 (very stable).

The ABL field measurements are seldom free from mesoscale disturbances, wave activities and nonstationarities. The situation could be further aggravated by several kinds of sensor errors (e.g., random spikes, amplitude resolution errors, drop outs, discontinuities), and stringent quality control and preprocessing of field data is of the utmost importance for any rigorous statistical analysis. Our quality control and preprocessing strategies are qualitatively similar to the suggestions of Vickers and Mahrt (1997) and Mahrt (1998b). Specifically, we follow these steps:

(1) Visual inspection of individual data series for the detection of spikes, amplitude resolution errors, drop outs and discontinuities is made. Suspected data series are discarded from further analyses.
(2) Adjustment is made for changes in wind direction by aligning sonic anemometer data using 60-s local averages of the longitudinal and transverse components of velocity.
(3) Partitioning of turbulent-mesoscale motion using discrete wavelet transform (Symmlet-8 wavelet) with a gap-scale (Vickers and Mahrt, 2003) of 100 s (see Figure 1 for an illustration) is carried out. Mesoscale motions (e.g., gravity waves, drainage flows) do not obey similarity theory and should be removed from the turbulent fluctuations when studying similarity relationships (Vickers and Mahrt, 2003). Vickers and Mahrt (2003) developed a Haar wavelet based automated algorithm to detect 'cospectral gap-scale' – the time scale that separates the turbulent and mesoscale transports. They found that under near-neutral conditions the gap-scale is approximately 500 s, but sharply decreases with increasing stability to as low as 30 s.

Since the determination of the gap-scales is not free from ambiguity, in this study we decided to work with a fixed gap-scale of 100 s. The selection of this particular time scale is entirely based on the past literature usage. Many researchers (e.g., Nieuwstadt, 1984b; Smedman, 1988; Forrer

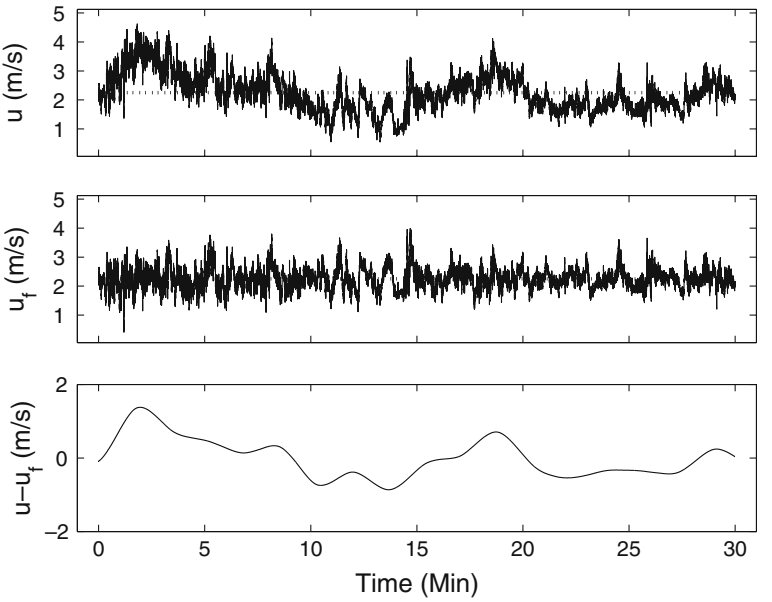

Figure 1. An illustration of the wavelet-based turbulent-mesoscale motion partitioning. Longitudinal (after alignment) velocity time series (u) observed during the Davis-99 field campaign (top); the same velocity series (u_f) after wavelet filtering (middle); and the mesoscale contamination ($u - u_f$) (bottom). The dotted line represents the mean velocity over 30-min period.

and Rotach, 1997, inter alia) have long been advocating the use of high-pass filtering of stably stratified turbulence data using a cut-off frequency of 0.01 Hz. This particular choice was based on the evidence of a spectral gap (minimum) at 0.01 Hz reported by Caughey (1982). Instead of Fourier based high-pass filtering, for the turbulent-mesoscale partitioning we used discrete wavelet transform. The excellent localization properties of the wavelet basis make it a preferable candidate over the Fourier basis.

(4) Finally, to check for nonstationarities of the partitioned series, we performed the following step: we subdivided each series in six equal intervals and computed the standard deviation of each sub-series (σ_i, $i = 1:6$). If $\max(\sigma_i)/\min(\sigma_i) > 2$, the series was discarded.

All the above steps were performed for all the three components of velocity (u, v, w) and temperature (θ), except that the nonstationarity check (step 4) was not performed on the v series. This choice was made to ensure that we have a sufficient number of runs for robust statistical analysis. After all these quality control and preprocessing steps were applied, we were left with 358 'reliable' sets of runs (out of an initial total of 633 runs) for testing the local scaling hypothesis.

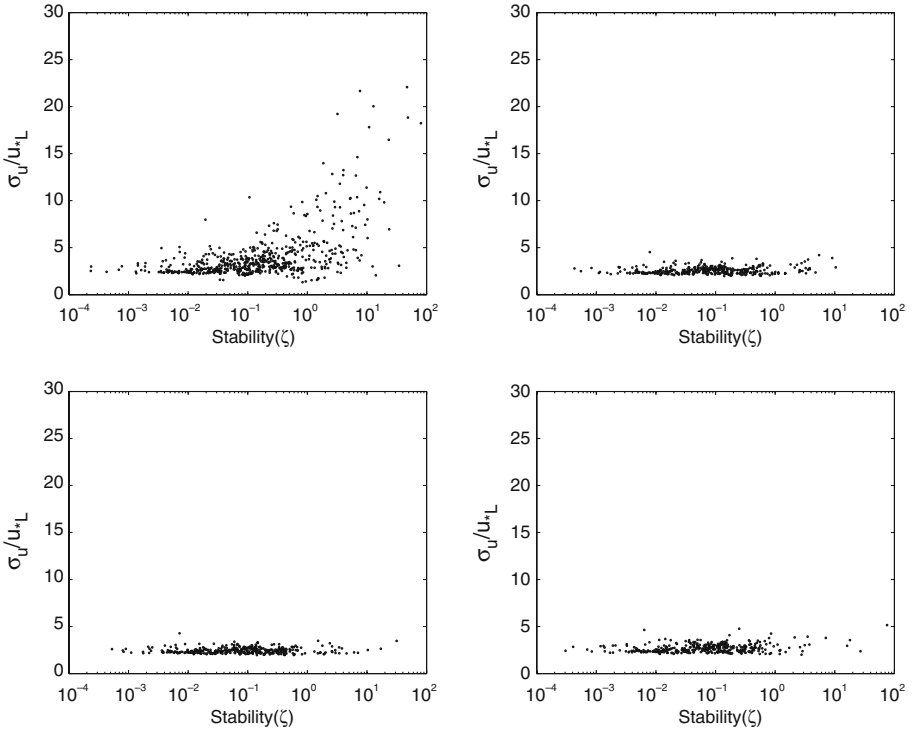

Figure 2. $\sigma_u/u_{*\mathrm{L}}$ versus stability (ζ) from field measurements without quality control and preprocessing (top-left), and the same measurements with appropriate quality control and preprocessing (gap-scale = 100 s) (top-right). The bottom figures also correspond to the same measurements with quality control and preprocessing but with gap-scales of 50 and 200 s, respectively. It is evident that the results are quite insensitive to the range of gap-scales considered here.

Figure 2 portrays the consequences of rigorous quality control and preprocessing steps on inferences about the validity of the local scaling hypothesis. The figure on the top-left, representing the case without quality control and preprocessing (only alignment was done), closely resembles Figure 1 of Pahlow et al., (2001) as expected (since the bulk of the data used in this study were also used by Pahlow et al., (2001)). On the other hand, the figures on the top-right, bottom-left and bottom-right strongly support the validity of the local scaling hypothesis, as well as the concept of z-less stratification. Later on, in Section 5, based on extensive analysis of different sources of data, we will argue that the conclusions of Pahlow et al., (2001) regarding the invalidity of local scaling and z-less stratifications under very stable conditions are biased by the inclusion of non-turbulent motions.

To substantiate this claim, we also utilized nine runs (corresponding to different levels of stratification) from the state-of-the-art wind-tunnel experiment of Ohya (2001) and simulations using a new-generation LES model (Porté-Agel et al., 2000; Porté-Agel, 2004; Stoll and Porté-Agel, 2006; Basu, 2004) in conjunction with the field datasets. It is noted that the field measurements we considered in this study essentially represent the surface layer; on the other hand, the wind-tunnel measurements and LES data comprise both the surface layer and the outer layer. This endows us with an excellent opportunity to test the local scaling hypothesis, since it is supposed to be valid for the entire boundary layer. However, the influence of boundary-layer height cannot be completely ignored near the top of the boundary layer. Note that the theoretical model of Nieuwstadt (1985) predicts singular behaviour near the boundary-layer top. Also, this is the most sensitive location where most of the LES models considered in the GABLS intercomparison differ from each other in terms of the blending of the SBL temperature profile with the overlying inversion (Beare et al., 2006). For these reasons, we considered data from the lowest 75% of the boundary layer (in the case of both wind-tunnel experiments and LES). Moreover, to avoid errors arising from flux measurement uncertainties, wind-tunnel measurements were further restricted such as to satisfy the following constraints: $u_{*\mathrm{L}} \geq 0.01\,\mathrm{m\,s^{-1}}$ and $|\overline{w\theta}_{\mathrm{L}}| \geq 0.001\mathrm{m\,K\,s^{-1}}$.

We would like to point out that the wind-tunnel measurements of Ohya (2001) displayed a non-traditional upside-down character, where turbulence is generated in the outer boundary layer rather than at the surface. In a recent study, Mahrt and Vickers (2002) mentioned that even though such a boundary layer is physically different from the traditional bottom-up boundary layer, the existence of local scaling in this boundary layer cannot be ruled out. Later, in Section 5, we show that this is indeed the case, i.e., the local scaling and z-less features are also found in the upside-down boundary layer.

4. Large-Eddy Simulation of the SBL

It has to be emphasized that field observations from the stably stratified boundary layer become increasingly uncertain with an increase in stability. This inevitable limitation highlights the need for simulated high-resolution spatio-temporal information about these highly stratified flows to supplement the observations. With the recent developments in computing resources, large-eddy simulations of turbulent flows in the ABL have the potential to provide this kind of information. However, until now LES models have not been sufficiently faithful in reproducing the characteristics of the very stable atmospheric boundary layer (Saiki et al., 2000;

Holtslag, 2003). The main weakness of LES is associated with our limited ability to accurately account for the dynamics that are not explicitly resolved in the simulations (because they occur at scales smaller than the grid size). Under very stable conditions – due to strong flow stratification – the characteristic size of the eddies becomes increasingly smaller with increase in atmospheric stability, which eventually imposes an additional burden on the LES subgrid-scale models. Furthermore, the recent GABLS LES intercomparison study (Beare et al., 2006) highlights that the LES of the moderately stable boundary layer is quite sensitive to SGS models at a relatively fine resolution of 6.25 m. At a coarser resolution (12.5 m) two traditional SGS model-based simulations resulted in unrealistic near-linear (without any curvature) temperature profiles. Sometimes, in these coarse-grid simulations, the SGS contributions to the total momentum or heat fluxes also became unreasonably high (much larger than 50%) in the interior of the boundary layer. These breakdowns of traditional SGS models undoubtedly call for improved SGS parameterizations in order to make LES a more reliable tool to study the very stable boundary layer.

As a first step towards this goal, we utilized a new-generation SGS scheme – the 'scale-dependent dynamic' model (Porté-Agel et al., 2000; Porté-Agel, 2004) – to simulate the moderately stable boundary layer at a relatively coarse resolution. In previous studies (Porté-Agel et al., 2000; Porté-Agel, 2004), the performance of this model in simulating the neutral boundary layer (with passive scalars) was found to be superior (in terms of proper near-wall SGS dissipation behaviour and velocity spectra) compared to the commonly used SGS models. Technical details of the scale-dependent SGS modelling have been exhaustively described in Porté-Agel et al. (2000) and Porté-Agel, (2004). To avoid repetition, we briefly present below the basic philosophy of this SGS modelling approach.

Eddy viscosity (eddy-diffusion) models are the most popular SGS models for LES of the ABL. They parameterize the SGS stresses (fluxes) as being proportional to the resolved velocity (temperature) gradients and involve two unknown coefficients, the so-called Smagorinsky coefficient and the SGS Prandtl number. The values of these coefficients are well established for homogeneous, isotropic turbulence. However, to account for shear effects in the ABL (due to near-wall effects and stable stratification), traditionally the eddy-viscosity modelling involves appropriate tuning of these coefficients, along with the use of various types of ad-hoc corrections – wall-damping and stability-correction functions (Mason, 1994).

An alternative approach is to use the 'dynamic' SGS modelling approach (Germano et al., 1991; Lilly, 1992). The dynamic model computes the values of these unknown eddy-viscosity (eddy-diffusion) model coefficients at every Time and Location in a flow field using the notion of scale similarity. Basically, the dynamic model avoids the need for a-priori specification

and consequent tuning of any SGS model coefficient because it is evaluated directly from the resolved scales in the LES.

In a recent work, by relaxing the implicit assumption of scale invariance in the dynamic modelling approach, Porté-Agel et al. (2000) proposed an improved and more generalized version of the dynamic model: the 'scale-dependent dynamic' SGS model. In a later work by Porté-Agel (2004), the same scale-dependent dynamic procedure was applied to estimate the SGS scalar flux. In essence this procedure not only eliminates the need for any ad-hoc assumption about the stability dependence of the SGS Prandtl number, but also completely decouples the SGS flux estimation from SGS stress computation, which is highly desirable.

4.1. Description of the LES code

In this work, we have used a modified version of the LES code described in Albertson and Parlange (1999), Porté-Agel et al. (2000), and Porté-Agel (2004). The salient features of this code are as follows:

- It solves the filtered Navier–Stokes equations written in rotational form (Orszag and Pao, 1974).
- Derivatives in the horizontal directions are computed using the Fourier co-location method, while vertical derivatives are approximated with second-order central differences (Canuto et al., 1988).
- De-aliasing of the nonlinear terms in Fourier space is done using the 3/2 rule (Canuto et al., 1988).
- The explicit second-order Adams–Bashforth time advancement scheme is used (Canuto et al., 1988).
- The scale-dependent dynamic SGS model with spectral cut-off filtering is used. The ratio between the filter width and grid spacing is set to two. The model coefficients are obtained dynamically by averaging locally on the horizontal plane with a stencil of three by three grid points following the approach of Zang et al. (1993). Mathematically more rigorous local models were also proposed in the literature (Piomelli and Liu, 1995; Ghosal et al., 1995). Their capabilities in the stably stratified atmospheric boundary-layer simulations have yet to be tested.
- The scale-dependence coefficients are determined dynamically over horizontal planes following Porté-Agel et al. (2000), and Porté-Agel (2004).
- Stress/flux free upper boundary condition is used.
- Monin–Obukhov similarity based lower boundary condition is used.
- Periodic lateral boundary condition is used.
- Coriolis terms involving horizontal wind are used.
- Forcing is imposed by the geostrophic wind.
- There is a Rayleigh damping layer near the top of the domain.

4.2. Description of simulation

In this work, we simulated the GABLS intercomparison case study utilizing the scale-dependent dynamic SGS model. This case study is described in detail in Beare et al. (2006). Briefly, the boundary layer is driven by an imposed, uniform geostrophic wind ($G = 8\,\mathrm{m\,s^{-1}}$), with a surface cooling rate of 0.25 K per hour and attains a quasi-steady state in $\approx$ 8–9 h with a boundary-layer depth of $\approx$200 m. The initial mean potential temperature was 265 K up to 100 m with an overlying inversion of strength $0.01\,\mathrm{K\,m^{-1}}$. The Coriolis parameter was set to $f_c = 1.39 \times 10^{-4}\,\mathrm{s^{-1}}$, corresponding to latitude 73° N. Our domain size was: ($L_x = L_y = L_z = 400$ m); this domain was divided into: (1) $N_x \times N_y \times N_z = 32 \times 32 \times 32$ nodes (i.e., $\Delta_x = \Delta_y = \Delta_z = 12.5$ m); (2) $N_x \times N_y \times N_z = 64 \times 64 \times 64$ nodes (i.e., $\Delta_x = \Delta_y = \Delta_z = 6.25$ m); and (3) $N_x \times N_y \times N_z = 80 \times 80 \times 80$ nodes (i.e., $\Delta_x = \Delta_y = \Delta_z = 5$ m). One of the objectives behind these simulations was to investigate the sensitivity of our results on grid resolution.

The lower boundary condition is based on the Monin–Obukhov similarity theory. The instantaneous wall shear stress $\tau_{i3,w}$ is represented as a function of the resolved velocity $\tilde{u}_i$ at the grid point immediately above the surface (i.e., at a height of $z = \Delta_z/2$ in our case):

$$\tau_{i3,w} = -u_*^2 \left[\frac{\tilde{u}_i(z)}{U(z)} \right] \quad (i = 1, 2), \tag{1}$$

where u_* is the friction velocity, which is computed from the mean horizontal mean velocity $U(z) = \langle (\tilde{u}_1^2 + \tilde{u}_2^2)^{1/2} \rangle$ at the first model level ($z = \Delta_z/2$) as follows:

$$u_* = \frac{U(z)\kappa}{\log(\frac{z}{z_o}) + \beta_m \frac{z}{L}}. \tag{2}$$

In a similar manner, the heat flux is computed as:

$$\overline{w\theta} = \frac{u_* \kappa \left[\theta_s - \Theta(z)\right]}{\log(\frac{z}{z_o}) + \beta_h \frac{z}{L}}, \tag{3}$$

where θ_s and $\Theta(z)$ denote the surface temperature and the mean resolved potential temperature at the first model level, respectively. Following the recommendations of the GABLS intercomparison study, the constants β_m and β_h were set to 4.8 and 7.8, respectively.

5. Results

The mean profiles of wind speed, potential temperature, momentum flux and heat flux, averaged over the final hour (8–9 h) of simulation, are shown

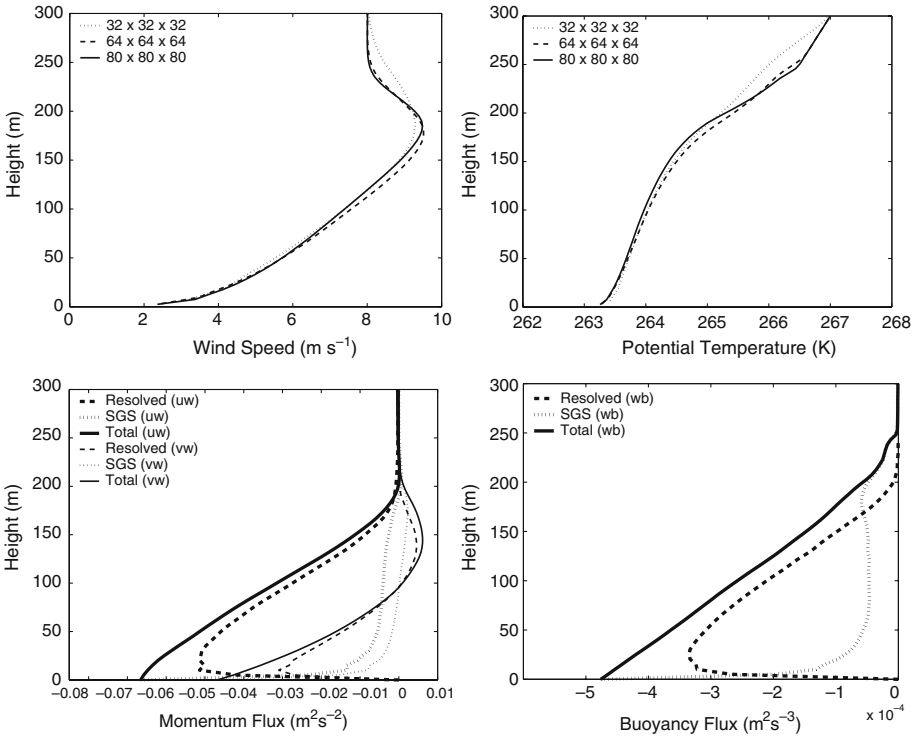

Figure 3. Mean wind speed (top-left) and potential temperature profiles (top right) for four different resolutions. Momentum flux (bottom-left) and heat flux (bottom-right) profiles correspond to the $80 \times 80 \times 80$ simulation. These profiles are averaged over the last one hour of simulation.

in Figure 3. The shapes and features of these profiles (e.g., super-geostrophic nocturnal jet near the top of the boundary layer, linear heat flux profile) are in accordance with Nieuwstadt's theoretical model for the 'stationary' stable boundary layer (Nieuwstadt, 1985) and also very similar to the fine-resolution simulations described in the GABLS LES intercomparison study (Beare et al., 2006).

The boundary-layer height[1] (H), Obukhov length (L) and other characteristics of the simulated SBL (averaged over the final hour of simulation) are given in Table I. From this table and also from Figure 3, it is apparent that the simulated (bulk) boundary-layer parameters are quite insensitive to the grid resolution. In LES this behaviour is always desirable and its existence is usually attributed to the validity of the SGS model. Whether or not the simulated turbulence statistics support the local scaling hypothesis will be discussed shortly. The LES statistics are computed from

[1] Following (Kosović and Curry, 2000; Beare et al., 2006), the boundary-layer height is defined as (1/0.95) times the height where the mean local stress falls to five percent of its surface value.

TABLE I

Basic characteristics of the simulated SBL during the last hour of simulation.

Grid points	h (m)	L (m)	u_* (m s^{-1})	θ_* (K)
$32 \times 32 \times 32$	205	113	0.283	0.047
$64 \times 64 \times 64$	185	114	0.276	0.045
$80 \times 80 \times 80$	192	122	0.285	0.045

TABLE II

Number of samples in each stability class.

Class	Stability (ζ)	Field observations	Wind-tunnel measurements	Large-eddy simulations
S1	0.00–0.10	200	15	3
S2	0.10–0.25	70	11	6
S3	0.25–0.50	41	24	8
S4	0.50–1.00	23	20	11
S5	> 1.00	24	7	33

the last one hour of the simulation, and all statistics are computed in the original model frame of reference. Small corrections due to wind rotation have been neglected. In the scale-dependent dynamic modelling approach, one does not solve additional prognostic equations for the SGS turbulence kinetic energy (TKE) and the SGS scalar variance. Thus, in order to estimate the SGS contributions to the total standard deviations, we followed the approach of Mason (1989) and Mason and Derbyshire (1990).

For ease in representation, we categorize our entire database based on local stabilities (z/Λ) (see Table II). The class S1 represents near neutral stability, while S5 corresponds to the very stable regime. We would like to point out that most of the very stable samples in the large-eddy simulations come from the interior of the boundary layer, rather than the surface layer. This is actually preferable from an LES perspective since the influences of the SGS terms significantly diminish away from the surface layer.

In Figures 4, 5, 6 and 7 we plot the normalized standard deviation of turbulent variables. The results are presented using standard boxplot notation with marks at 95, 75, 50, 25, and 5 percentile of an empirical distribution. Please note that the Figures 2 (top-right) and 4 represent the same results in two different formats.

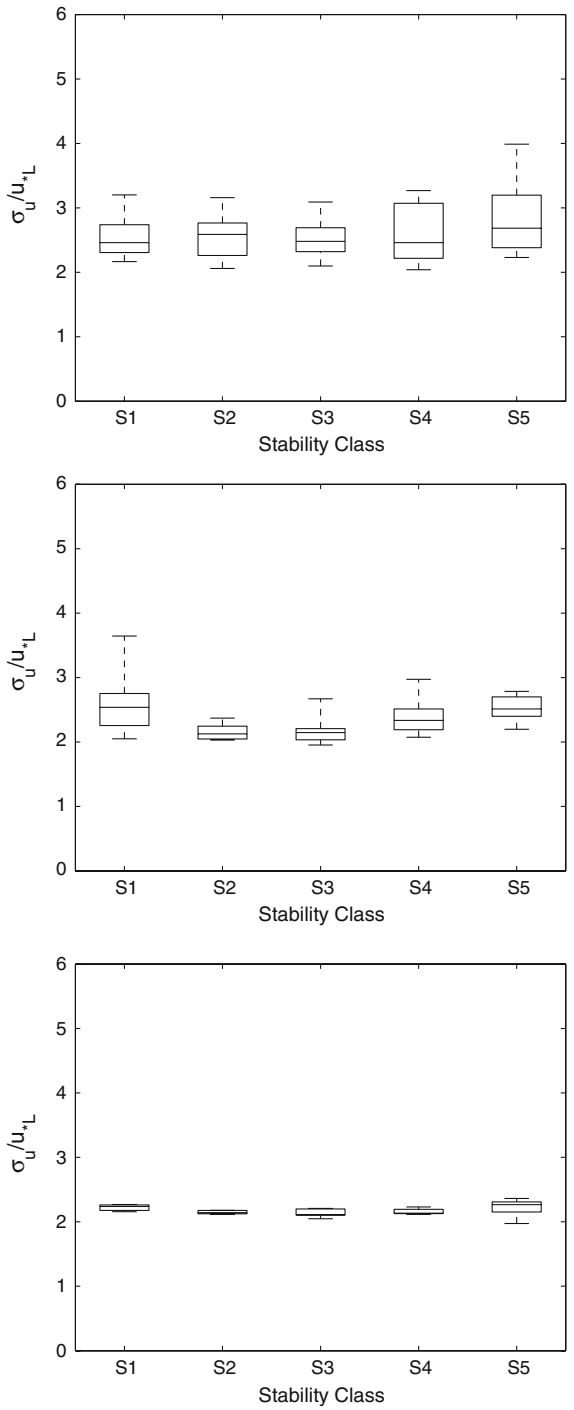

Figure 4. $\sigma_u/u_{*\mathrm{L}}$ from field measurements (top), wind-tunnel measurements (middle), and large-eddy simulations (bottom).

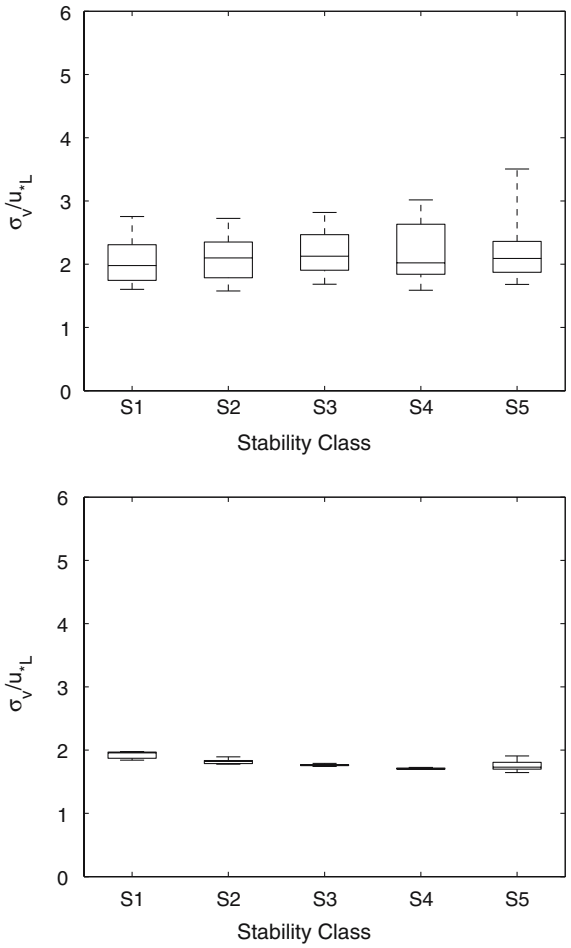

Figure 5. $\sigma_v/u_{*\mathrm{L}}$ from field measurements (top), and large-eddy simulations (bottom).

It is quite evident from Figures 4 to 7 that the normalized standard deviation of the turbulence variables closely follows the local scaling predictions and also z-less stratification. In Table III we further report the median values of the turbulence statistics corresponding to the category S5. Loosely, these median values could be considered as the asymptotic z-less values, which are found to be remarkably close to Nieuwstadt's analytical predictions and also his field observations (see Table III). For example, Nieuwstadt's theory predicts that the normalized vertical velocity standard deviation asymptotically approaches ≈ 1.4 in the z-less regime. In the present study, we observe this value to be in the narrow range of 1.4–1.6. Recently, Heinemann (2004) compiled a list (see Table II of his paper) of turbulence statistics under very stable conditions ($\zeta_{\max} \approx 25$) reported by

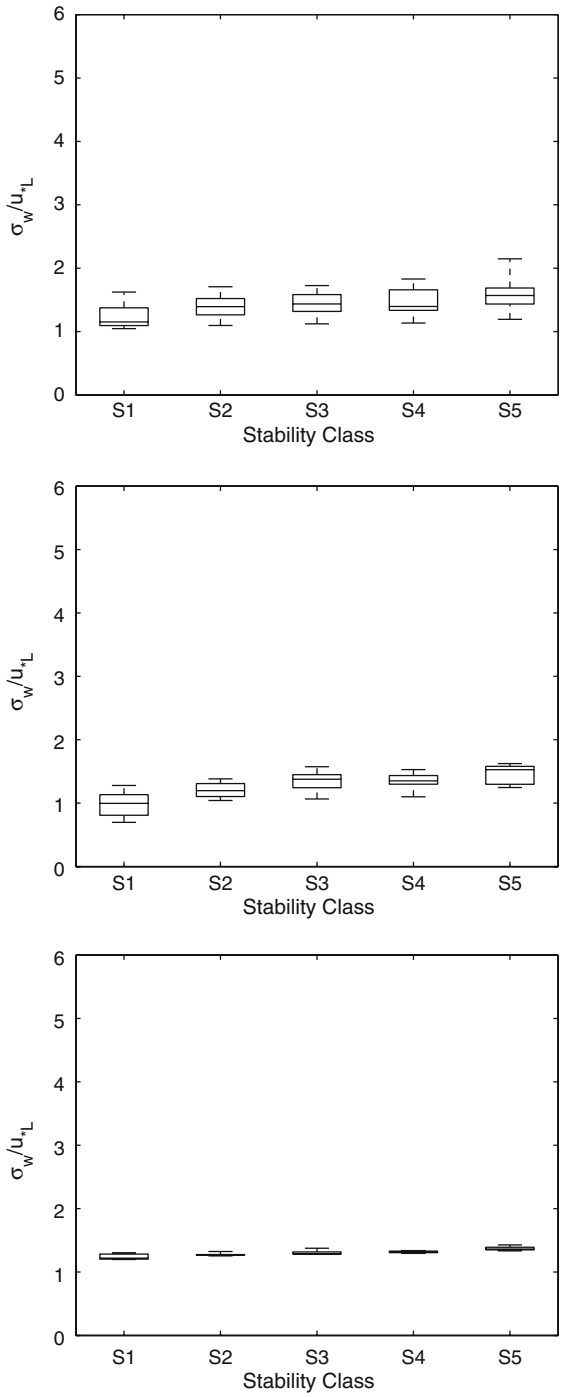

Figure 6. $\sigma_w/u_{*\mathrm{L}}$ from field measurements (top), wind-tunnel measurements (middle), and large-eddy simulations (bottom).

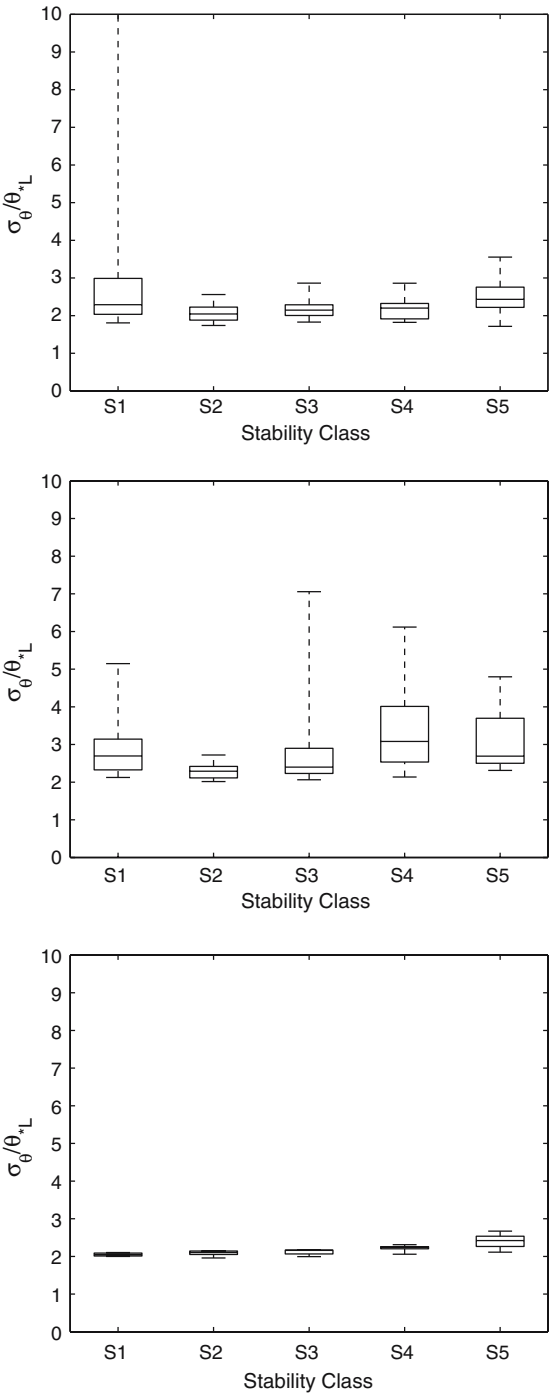

Figure 7. $\sigma_\theta/\theta_{*\mathrm{L}}$ from field measurements (top), wind-tunnel measurements (middle), and large-eddy simulations (bottom).

TABLE III
Median z-less values of turbulence statistics.

Turbulence statistics	Field observations	Wind-tunnel measurements	Large-eddy simulations	Nieuwstadt (1984b, 1985)
σ_u/u_{*L}	2.7	2.5	2.3	2.0
σ_v/u_{*L}	2.1	–	1.7	1.7
σ_w/u_{*L}	1.6	1.5	1.4	1.4
$\sigma_\theta/\theta_{*L}$	2.4	2.7	2.4	3.0
r_{uw}	−0.21	−0.28	−0.32	–
$r_{u\theta}$	0.51	0.55	0.56	–
$r_{w\theta}$	−0.27	−0.24	−0.30	−0.24

various researchers, and found an asymptotic value of ≈ 1.6 for $\sigma_w/u_{*\mathrm{L}}$. These results should be contrasted with Figure 3 of Pahlow et al. (2001).

Next, we plot the downward heat flux profiles in Figure 8. In the very stable regime (class S5) due to suppression of turbulence, the heat flux vanishes (Mahrt, 1998a). Of course, the heat flux should also go to zero in the near-neutral limit (class S1) since the temperature fluctuations become quite small. The maximum downward heat flux occurs in between these two extremes. Mahrt (1998a) reported that this maximum flux occurs at $\zeta = 0.05$ based on Microfronts data, whereas Mahli (1995) found ζ to be 0.20. In the literature, there is no general consensus on this value and also from Figure 8 it is quite difficult to estimate. The wind-tunnel measurements show that the maximum heat flux occurs in the stability class S2 (i.e., $\zeta = 0.10 - 0.25$), which would support Mahli's result. However, the field measurements would definitely be in favour of Mahrt (1998a).

It is widely accepted that as the stability increases the turbulent fluxes become increasingly intermittent (Mahrt, 1989). One way to quantify the degree of flux intermittency is the use of the so-called intermittency factor (IF), introduced by Howell and Sun (1999). To compute IF, first one needs to divide individual time series of u, v, w and θ into N smaller subrecords (in this work $N = 20$, which corresponds to 1.5-min windows for 30-min signals and so on). Subsequently, local fluxes (F_i) are computed from the deviation of subrecord averages. If M subrecords are needed such that the ratio of $\sum_{i=1}^{M} F_i$ to $\sum_{i=1}^{N} F_i$ exceeds 0.9, then the intermittency factor is simply defined as: $\mathrm{IF} = 1 - M/N$. In the asymptotic limit of $M \to N$, i.e., when the turbulent fluxes are uniformly distributed, IF goes to zero. On the other hand, if $M \to 1$, then the intermittency factor approaches unity. From the field measurements we compute the intermittency factors for

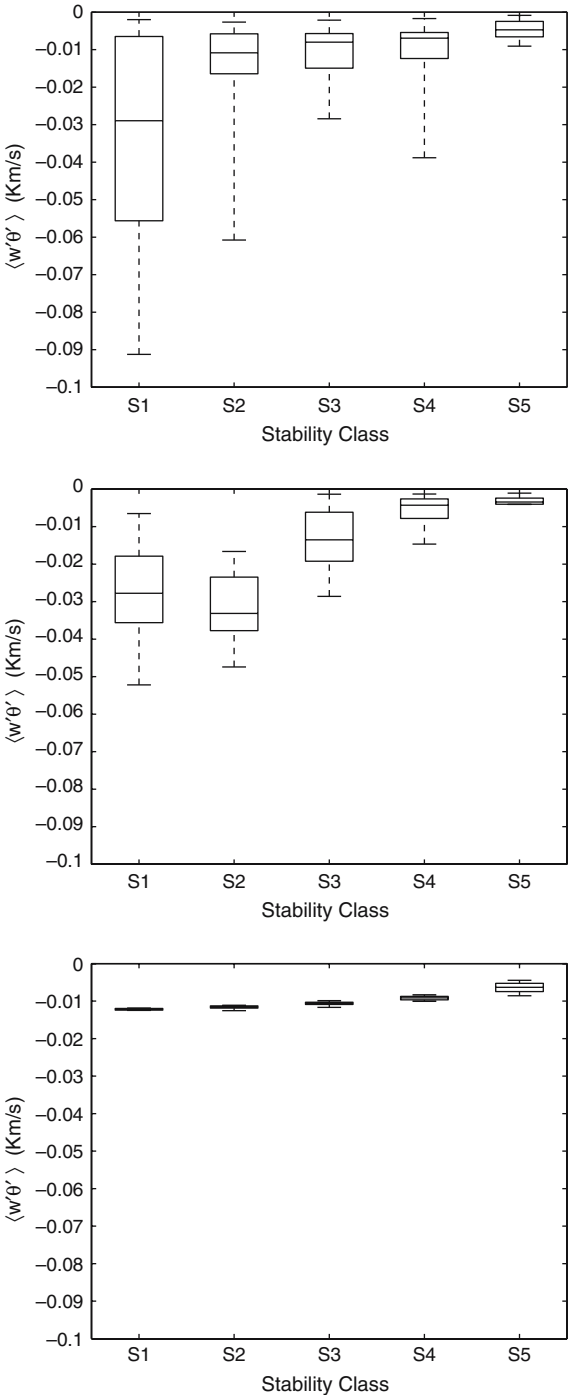

Figure 8. Heat flux ($\overline{w\theta}$) (m K s^{-1}) from field measurements (top), wind-tunnel measurements (middle), and large-eddy simulations (bottom).

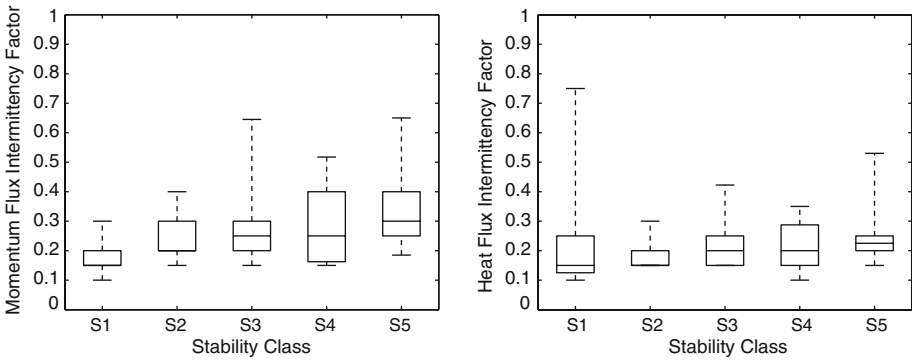

Figure 9. Intermittency factors corresponding to momentum fluxes (left), and heat fluxes (right) derived from field measurements.

vertical momentum ($\overline{uw}$) and heat fluxes ($\overline{w\theta}$) (see Figure 9). For the entire stability range the IFs are greater than zero. For the momentum flux, the increase of intermittency with increasing stability is quite clear. In the case of the heat flux the intermittency increases in both the near-neutral (S1) and very stable (S5) regimes. In the near-neutral regime the temperature fluctuations are very small and the computation of very weak heat flux becomes problematic and leads to significant intermittency.[2] The increase in IF in the case of S5 is definitely a signature of the intermittent very stable boundary layer.

In Figures 10, 11 and 12, we report the mutual correlations between u, w and θ. The z-less values are also reported in Table III. Once again, these values are very similar to those compiled by Heinemann (2004) and theoretical predictions of Nieuwstadt (1984b). As a note, Kaimal and Finnigan (1994) also report that for $0 < \zeta < 1, r_{u\theta} = 0.6$, which is close to the values found in the present study (see Figure 11).

Lastly, in Figure 13 we plot the stability dependence of the nondimensionalized third-order moments ($\phi_{\theta\theta\theta} = \overline{\theta^3}/\theta_*^3, \phi_{w\theta\theta} = \overline{w\theta^2}/(u_*\theta_*^2)$, and $\phi_{ww\theta} = \overline{ww\theta}/(u_*^2\theta_*)$) derived from our field measurements database. Even though in the past several studies have provided evidence of local scaling in turbulence gradients and variances, results confirming its existence in the case of higher-order moments are quite rare in the literature, a notable exception being the study by Dias et al. (1995). They showed that these nondimensionalized third-order moments obey local scaling and essentially remain constant (~ 0) for the entire stability range considered. As evident from Figure 13, our present analysis definitely supports the conclusions of Dias et al. (1995).

[2] This intermittent near-neutral behaviour is also reflected in the plots of the variance and third-order moment of temperature (see Figures 7 and 13, respectively), as would be anticipated.

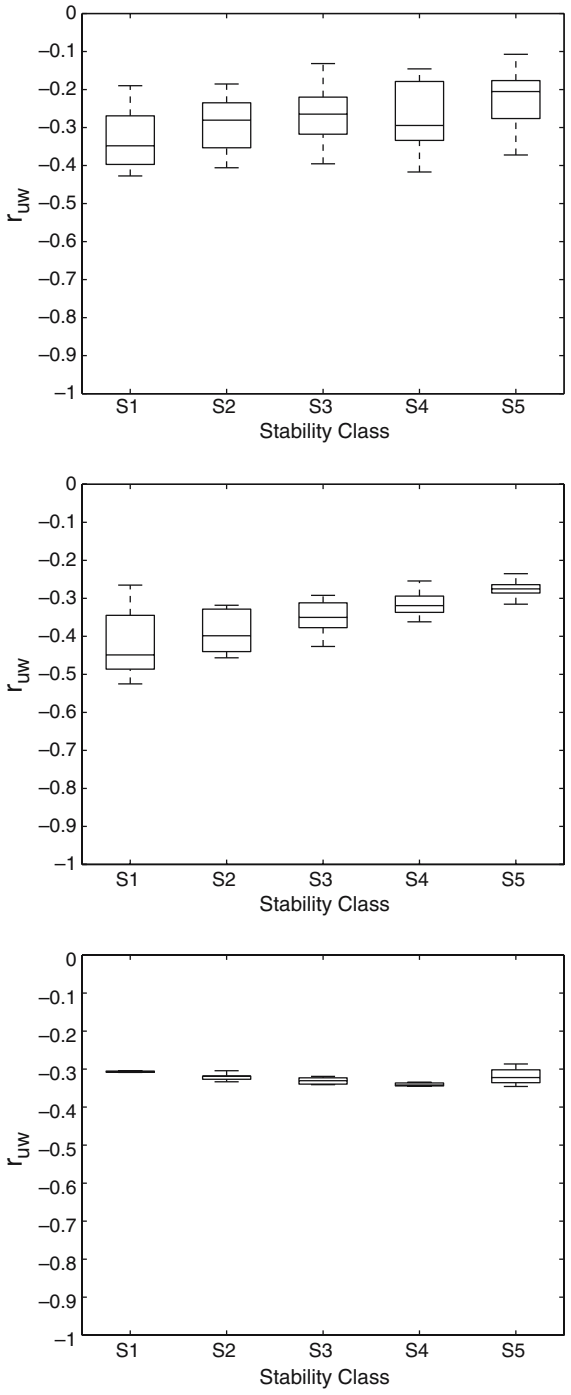

Figure 10. Correlation between u and w (r_{uw}) from field measurements (top), wind-tunnel measurements (middle), and large-eddy simulations (bottom).

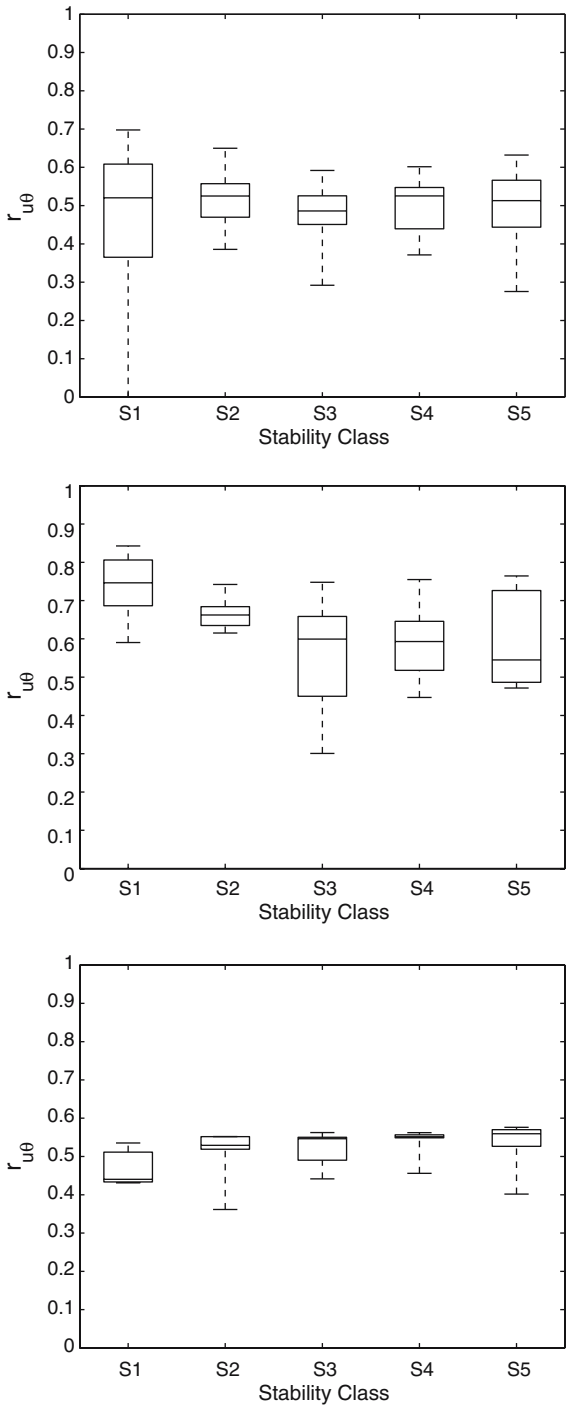

Figure 11. Correlation between u and θ ($r_{u\theta}$) from field measurements (top), wind-tunnel measurements (middle), and large-eddy simulations (bottom).

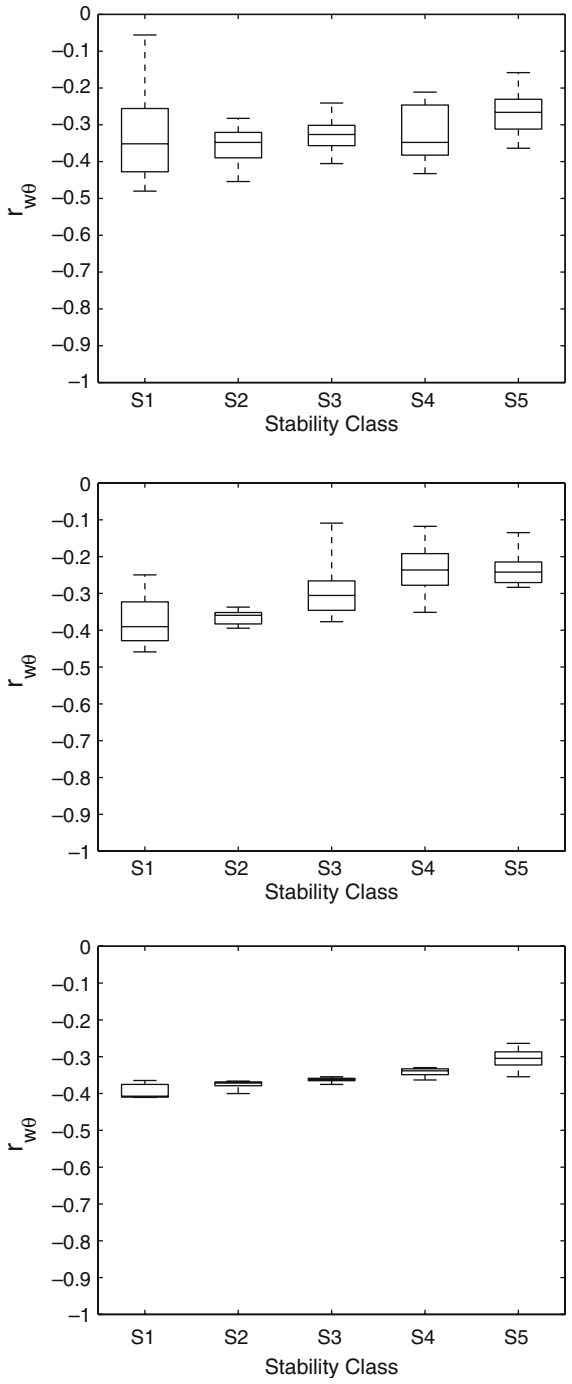

Figure 12. Correlation between w and θ ($r_{w\theta}$) from field measurements (top), wind-tunnel measurements (middle), and large-eddy simulations (bottom).

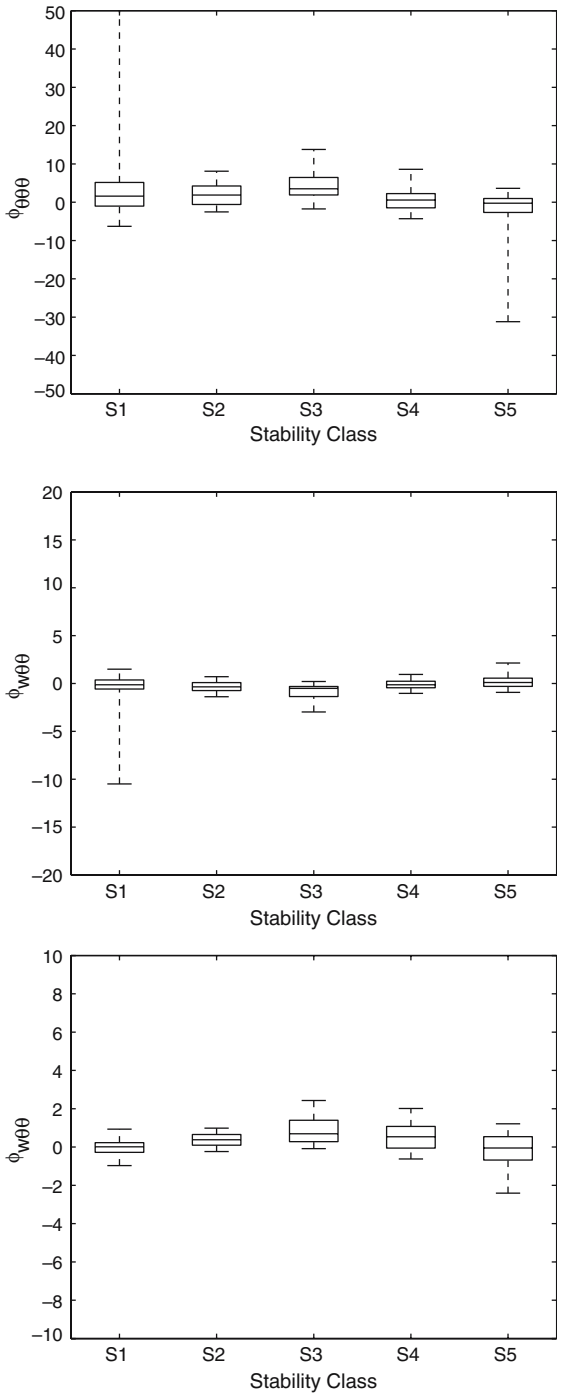

Figure 13. Nondimensionalized third-order moments: $\phi_{\theta\theta\theta}$ (top), $\phi_{w\theta\theta}$ (middle), and $\phi_{ww\theta}$ (bottom), obtained from field observations.

In light of the foregoing analyses and discussion it is certain that the local scaling hypothesis of Nieuwstadt, which has survived the last two decades, still holds for a wide range of stabilities provided that mesoscale motions are not included.

6. Summary

In this study, we performed rigorous statistical analyses of field observations and wind-tunnel measurements and also employed a new-generation large-eddy SGS model in order to verify the validity of Nieuwstadt's local-scaling hypothesis under very stable conditions. An extensive set of turbulence statistics, computed from field and wind-tunnel measurements and from LES generated datasets, supports the validity of the local scaling hypothesis (in the cases of traditional bottom-up as well as upside-down stable boundary layers over homogeneous, flat terrains). We demonstrate that non-turbulent effects need to be removed from field data while studying similarity hypotheses.

In a parallel work (Basu, 2004), we also found that the stability functions (commonly used in the first-order turbulent K-closure models) extracted from idealized LESs closely resemble the observational-based M–O stability functions (Basu, 2004). These kinds of agreements between our simulated results and field observations are very encouraging. They not only provide more confidence in our results but also highlight the credibility of the scale-dependent dynamic SGS modelling approach in simulating the stable boundary layer.

Acknowledgements

Special thanks go to Yuji Ohya for sending us his state-of-the-art wind-tunnel data. We are grateful to all those researchers who painstakingly collected data during the Iowa, Davis and CASES-99 field campaigns. We greatly acknowledge the valuable comments and suggestions made by Rob Stoll during the course of this study. This work was partially funded by NSF (EAR-0094200 and EAR-0120914 as part of the National Center for Earth-surface Dynamics) and NASA (NAG5-12909, NAG5-13639, NAG5-10569 and NAG5-11801) grants. One of us (SB) was partially supported by the Doctoral Dissertation Fellowship from the University of Minnesota. All the computational resources were kindly provided by the Minnesota Supercomputing Institute.

References

Albertson, J. D. and Parlange, M. B.: 1999, 'Natural Integration of Scalar Fluxes from Complex Terrain', *Adv. Wat. Res.* **23**, 239–252.

Andrén, A.: 1995, 'The Structure of Stably Stratified Atmospheric Boundary Layers: A Large-Eddy Simulation Study', *Quart. J. Roy. Meteorol. Soc.* **121**, 961–985.

Arya, S. P.: 2001, *Introduction to Micrometeorology*, Academic Press, San Diego, CA, 420 pp.

Barnard, J. C.: 2000, 'Intermittent Turbulence in the Very Stable Ekman Layer', PhD Thesis, Department of Mechanical Engineering, University of Washington, 154 pp.

Basu, S., Foufoula-Georgiou, E., and Porté-Agel, F.: 2002, 'Predictability of Atmospheric Boundary-layer Flows as a Function of Scale', *Geophys. Res. Lett.* **29**, doi:10.1029/2002GL015497.

Basu, S.: 2004, 'Large-Eddy Simulation of Stably Stratified Atmospheric Boundary Layer Turbulence: A Scale-Dependent Dynamic Modeling Approach', PhD Thesis, Department of Civil Engineering, University of Minnesota, 114 pp.

Beare, R. J. and MacVean, M. K.: 2004, 'Resolution Sensitivity and Scaling of Large-Eddy Simulations of the Stable Boundary Layer', *Boundary-Layer Meteorol.* **112**, 257–281.

Beare, R. J. et al.: 2006, 'An Intercomparison of Large-Eddy Simulations of the Stable Boundary Layer', *Boundary-Layer Meteorol.* **118**, xx-xx.

Beljaars, A.: 1992, 'The Parameterization of the Planetary Boundary Layer', *ECMWF Meteorological Training Course Lecture Series*, 1–57.

Beljaars, A. and Viterbo, P.: 1998, 'The Role of the Boundary Layer in a Numerical Weather Prediction Model', in A. A. M. Holtslag and P. G. Duynkerke (eds.), *Clear and Cloudy Boundary Layers*, Royal Netherlands Academy of Arts and Sciences, Amsterdam, pp. 297–304.

Brown, A. R., Derbyshire, S. H, and Mason, P. J.: 1994, 'Large-Eddy Simulation of Stable Atmospheric Boundary Layers with a Revised Stochastic Subgrid Model', *Quart. J. Roy. Meteorol. Soc.* **120**, 1485–1512.

Canuto, C., Hussaini, M. Y., Quarteroni, A., and Zhang, T. A.: 1988, *Spectral Methods in Fluid Dynamics*, Springer Verlag, Berlin, Germany, 557 pp.

Caughey, S. J.: 1982, 'Observed Characteristics of the Atmospheric Boundary Layer', in F. T. M. Nieuwstadt and H. van Dop (eds.), *Atmospheric Turbulence and Air Pollution Modelling*, D. Reidel Publishing Company, Dordrecht, pp. 107–158.

Cuxart, J., and Coauthors: 2000, 'Stable Atmospheric Boundary-Layer Experiment in Spain (SABLES 98): A Report', *Boundary-Layer Meteorol.* **96**, 337–370.

Derbyshire, S. H.: 1990, 'Nieuwstadt's Stable Boundary Layer Revisited', *Quart. J. Roy. Meteorol. Soc.* **116**, 127–158.

Derbyshire, S. H.: 1999, 'Stable Boundary-Layer Modelling: Established Approaches and Beyond', *Boundary-Layer Meteorol.* **90**, 423–446.

Dias, N. L., Brutsaert, W., and Wesely, M. L.: 1995, 'Z-Less Stratification under Stable Conditions', *Boundary-Layer Meteorol.* **75**, 175–187.

Ding, F., Arya, S. P., and Lin, Y.-L.: 2001, 'Large-Eddy Simulations of the Atmospheric Boundary Layer Using a New Subgrid-Scale Model: Part II. Weakly and Moderately Stable Cases', *Environ. Fluid Mech.* **1**, 49–69.

Forrer, J. and Rotach, M. W.: 1997, 'On the Turbulence Structure in the Stable Boundary Layer over the Greenland Ice Sheet', *Boundary-Layer Meteorol.* **85**, 111–136.

Galmarini, S., Beets, C., Duynkerke, P. G., and Vilà-Guerau de Arellano, J.: 1998, 'Stable Nocturnal Boundary Layers: A Comparison of One-dimensional and Large-eddy Simulation Models', *Boundary-Layer Meteorol.* **88**, 181–210.

Germano, M., Piomelli, U., Moin, P., and Cabot, W. H.: 1991, 'A Dynamic Subgrid-scale Eddy Viscosity Model', *Phys. Fluids A* **3**, 1760–1765.

Ghosal, S., Lund, T. S., Moin, P., and Akselvoll, K.: 1995, 'A Dynamic Localization Model for Large-Eddy Simulation of Turbulent Flows', *Phys. Fluids A* **3**, 1760–1765.

Heinemann, G.: 2004, 'Local Similarity Properties of the Continuously Turbulent Stable Boundary Layer over Greenland', *Boundary-Layer Meteorol.* **112**, 283–305.

Holtslag, A. A. M.: 2003, 'GABLS Initiates Intercomparison for Stable Boundary Layer Case', *GEWEX News* **13**, 7–8.

Howell, J. F. and Sun, J.: 1999, 'Surface-Layer Fluxes in Stable Conditions', *Boundary-Layer Meteorol.* **90**, 495–520.

Hunt, J. C. R., Shutts, G. J., and Derbyshire, S.: 1996, 'Stably Stratified Flows in Meteorology', *Dyn. Atmos. Oceans* **23**, 63–79.

Kaimal, J. C. and Finnigan, J. J.: 1994, *Atmospheric Boundary Layer Flows: Their Structure and Measurement*, Oxford University Press, Oxford, U.K., 289 pp.

Kosović, B. and Curry J. A.: 2000, 'A Large Eddy Simulation Study of a Quasi-Steady, Stably Stratified Atmospheric Boundary Layer', *J. Atmos. Sci.* **57**, 1052–1068.

Lilly, D. K.: 1992, 'A Proposed Modification of the Germano Subgrid-scale Closure Method', *Phys. Fluids A* **4**, 633–635.

Mahli, Y. S.: 1995, 'The Significance of the Dual Solutions for Heat Fluxes Measured by the Temperature Fluctuation Method in Stable Conditions', *Boundary-Layer Meteorol.* **74**, 389–396.

Mahrt, L.: 1989, 'Intermittency of Atmospheric Turbulence', *J. Atmos. Sci.* **46**, 79–95.

Mahrt, L.: 1998a, 'Stratified Atmospheric Boundary Layers and Breakdown of Models', *Theoret. Comput. Fluid Dyn.* **11**, 263–279.

Mahrt, L.: 1998b, 'Flux Sampling Errors for Aircraft and Towers', *J. Atmos. Oceanic Tech.* **15**, 416–429.

Mahrt, L. and Vickers, D.: 2002, 'Contrasting Vertical Structures of Nocturnal Boundary Layers', *Boundary-Layer Meteorol.* **105**, 351–363.

Mason, P.: 1989, 'Large-Eddy Simulation of the Convective Atmospheric Boundary Layer', *J. Atmos. Sci.* **46**, 1492–1516.

Mason, P.: 1994, 'Large-Eddy Simulation: A Critical Review of the Technique', *Quart. J. Roy. Meteorol. Soc.* **120**, 1–26.

Mason, P. J. and Derbyshire, S. H.: 1990, 'Large-Eddy Simulation of the Stably-Stratified Atmospheric Boundary Layer', *Boundary-Layer Meteorol.* **53**, 117–162.

McNider, R. T., England, D. E., Friedman, M. J., and Shi, X.: 1995, 'Predictability of the Stable Atmospheric Boundary Layer', *J. Atmos. Sci.* **52**, 1602–1614.

Monin, A. S. and Yaglom, A. M.: 1971, *Statistical Fluid Mechanics: Mechanics of Turbulence*, Vol. 1, MIT Press, Cambridge, MA, 769 pp.

Nieuwstadt, F. T. M.: 1984a, 'Some Aspects of the Turbulent Stable Boundary Layer', *Boundary-Layer Meteorol.* **30**, 31–55.

Nieuwstadt, F. T. M.: 1984b, 'The Turbulent Structure of the Stable, Nocturnal Boundary Layer', *J. Atmos. Sci.* **41**, 2202–2216.

Nieuwstadt, F. T. M.: 1985, 'A Model for the Stationary, Stable Boundary Layer', in J. C. R. Hunt (ed.), *Turbulence and Diffusion in Stable Environments*, Clarendon Press, Oxford, U.K., pp. 149–179.

Ohya, Y.: 2001, 'Wind-Tunnel Study of Atmospheric Stable Boundary Layers over a Rough Surface', *Boundary-Layer Meteorol.* **98**, 57–82.

Ohya, Y., Neff, D. E., and Meroney, R. N.: 1997, 'Turbulence Structure in a Stratified Boundary Layer under Stable Conditions', *Boundary-Layer Meteorol.* **83**, 139–161.

Orszag, S. A., and Pao, Y.-H.: 1974, 'Numerical Computation of Turbulent Shear Flows', *Adv. Geophys.* **18A**, 224–236.

Pahlow, M., Parlange, M. B., and Porté-Agel, F.: 2001, 'On Monin–Obukhov Similarity in the Stable Atmospheric Boundary Layer', *Boundary-Layer Meteorol.* **99**, 225–248.

Piomelli, U., and Liu, J.: 1995, 'Large-Eddy Simulation of Rotating Channel Flows using a Localized Dynamic Model', *Phys. Fluids* **7**, 839–848.

Porté-Agel, F., Meneveau, C., and Parlange, M. B.: 2000, 'A Scale-Dependent Dynamic Model for Large-Eddy Simulation: Application to a Neutral Atmospheric Boundary Layer', *J. Fluid Mech.* **415**, 261–284.

Porté-Agel, F.: 2004, 'A Scale-Dependent Dynamic Model for Scalar Transport in LES of the Atmospheric Boundary Layer', *Boundary-Layer Meteorol.* **112**, 81–105.

Poulos, G. S. and Coauthors: 2002, 'CASES-99: A Comprehensive Investigation of the Stable Nocturnal Boundary Layer', *Bull. Amer. Meteorol. Soc.* **83**, 555–581.

ReVelle, D. O.: 1993, 'Chaos and "Bursting" in the Planetary Boundary Layer', *J. Appl. Meteorol.* **32**, 1169–1180.

Saiki, E. M., Moeng, C.-H., and Sullivan, P. P.: 2000, 'Large-Eddy Simulation of the Stably Stratified Planetary Boundary Layer', *Boundary-Layer Meteorol.* **95**, 1–30.

Smedman, A.: 1988, 'Observations of a Multi-Level Turbulence Structure in a Very Stable Atmospheric Boundary Layer', *Boundary-Layer Meteorol.* **44**, 231–253.

Sorbjan, Z.: 1989, *Structure of Atmospheric Boundary Layer*, Prentice-Hall, Englewood Cliffs, NJ, 317 pp.

Stoll, R., and Porté-Agel, F.: 2006, 'Effect of Roughness on Surface Boundary Conditions for Large-eddy Simulation', *Boundary-Layer Meteorol.* **118**, xx-xx.

Stull, R. B.: 1988, *An Introduction to Boundary Layer Meteorology*, Kluwer Academic Publishers, Dordrecht, The Netherlands, 670 pp.

van de Wiel, B.: 2002, 'Intermittent Turbulence and Oscillations in the Stable Boundary Layer over Land', PhD Thesis, Wageningen University, Netherlands, 129 pp.

Vickers, D. and Mahrt, L.: 1997, 'Quality Control and Flux Sampling Problems for Tower and Aircraft Data', *J. Atmos. Oceanic Tech.* **14**, 512–526.

Vickers, D. and Mahrt, L.: 2003, 'The Cospectral Gap and Turbulent Flux Calculations', *J. Atmos. Oceanic Tech.* **20**, 660–672.

Viterbo, P., Beljaars, A., Mahfouf, J.-F., and Teixeira, J.: 1999, 'The Representation of Soil Moisture Freezing and its Impact on the Stable Boundary Layer', *Quart. J. Roy. Meteorol. Soc.* **125**, 2401–2426.

Wyngaard, J. C.: 1973, 'On Surface Layer Turbulence', in D. A. Haugen (ed.), *Workshop on Micrometeorology*, American Meteorological Society, Boston, pp. 109–149.

Zang, Y., Street, R. L., and Koseff, J. R.: 1993, 'A Dynamic Mixed Subgrid-scale Model and its Application to Turbulent Recirculating Flows', *Phys. Fluids. A* **5**, 3186–3196.